Directional preference of otolith-related neurons in vestibular nucleus

Nguyen Nguyen
Inha University College of Medicine
Kyu-Sung Kim
Inha University College of Medicine
Gyutae Kim (kgthee@gmail.com)
Inha University https://orcid.org/0000-0001-6747-8189

Research article

Keywords: Directional preference, Vestibular nucleus, Otolith-related neuron, Unilateral labyrinthectomy

Posted Date: August 7th, 2020

DOI: https://doi.org/10.21203/rs.3.rs-16440/v3

Abstract

Background: Due to the paired structure of two labyrinths, their neural communication is conducted through the interconnected commissural pathway. Using the tight link, the neural responding characteristics are formed in vestibular nucleus, and these responses are initially generated by the mechanical movement of the hair cells in the semicircular canals and otoliths. Although the mechanism to describe the neuronal responses to the head movements was evident, few direct experimental data were provided, especially the directional preference of otolith-related neurons as one of critical responses to elucidate the function of the neurons in vestibular nucleus (VN).

Experimental Approach: The directional preference of otolith-related neurons was investigated in VN. Also, a chemically induced unilateral labyrinthectomy (UL) was performed to identify the origin of the directional preference. For the model evaluation, static and dynamic behavioral tests were performed. Following the evaluation, an extracellular neural activity was recorded for the neuronal responses to the horizontal head rotation and the linear head translation.

Results: Seventy seven neuronal activities were recorded from thirty SD rats (270-450 g, male), and total population was divided into three groups; left UL (20), sham (35), right UL (22). Based on the directional preference, two sub-groups were again classified as contra- and ipsi-preferred neurons. There was no significance in the number of those sub-groups (contra-: 15/35, 43%; ipsi-: 20/35, 57%) in the sham ($p=0.155$). However, more ipsi-preferred neurons (19/22, 86%) were observed after right UL ($p=6.056\times10^{-5}$) while left UL caused more contra-preferred neurons (13/20, 65%) ($p=0.058$). In particular, the convergent neurons mainly led this biased difference in the population (ipsi-: 100% after right UL & contra-: 89% after left UL) ($p<0.002$).

Conclusion: The directional preference was evenly maintained under a normal vestibular function, and its unilateral loss biased the directional preference of the neurons, depending on the side of lesion. Moreover, the dominance of the directional preference was mainly led by the convergent neurons which had the neural information related with head rotation and linear translation.

Background

Vestibular nucleus (VN) is the core neural complex which receives input primarily from the peripheral vestibular organ as well as other different body structures, and the obtained messages are processed and converged in VN. As two labyrinths are separately positioned at both sides of the head, the generated vestibular information from the ipsilateral labyrinth initially projects on the ipsilateral VN, and it is again transferred to the contralateral VN through the interconnected commissural pathway (CP) [1-5]. Thus, if a unilateral vestibular loss occurs, the VN fails to receive the incoming sensation of head movement, and it results in imbalanced vestibular functions, such as balance control, head orientation, and navigation [6-8]. Vestibular dysfunction has been induced artificially by unilateral labyrinthectomy (UL) to assess the neural and behavioral effects by the unilateral vestibular loss [9-11]. For the detection of head movement,

three semicircular canals and two otoliths in each inner ear sense head rotation and linear translation, respectively. Especially, the otoliths generate the directional signals during the linear head translation, and the generated neural information supports a highly functional performance, like navigation [6]. The directional sensitivity of the vestibular neurons is determined by the hair cells in the canals and the otoliths. In each canal, afferent neurons have the same directional preference [12]. The morphological polarization of hair cells in a canal was triggered by the deflection of the cupula, and the direction for the neural excitation was same in all neurons of the canal. During the head rotation, the inhibitory direction in the ipsilateral VN became an excitatory information in the contralateral VN and vise versa for the balanced neural information at the separated VNs [13]. On the other hand, the otolithic organ has a relatively complicated organization in the generation of its directional signal. Anatomically, the otolithic surface is unequally divided by striola; approximately two thirds as the pars medialis and the rest as the pars lateralis, which have the opposite responses to a linear translation [14-17]. The uneven responses by different portions in the structure affect the neural information, and the dominant neural signal comes from the pars medialis [14,15].

Even though the underlying mechanism in the generation of the otolithic signals was well described, few experimental results showed the unbalanced distribution of the directional preference of otolith-related neurons after UL. According to a previous study, the directional preference of otolith-related neurons under a normal condition was biased to contra-direction [18]. However, this result was rarely supported by direct studies to identify the neural responding property (directional preference) during the head linear translation. Furthermore, it has been unknown what kind of neural information mainly leads the directional preference of the otolith-related neurons by unilateral vestibular loss. Here, the directional preference of the otolith-related neurons in VN was examined. Also, the neuronal responses were classified depending on the neural information, which was originated from pure (only otolith) or convergent neurons (both otolith and canal). To emphasize the obtained results, a UL model was constructed by an intratympanic toxic injection, and it was investigated how unilateral vestibular loss affected the directional preference in the otolith-related neurons.

Results

Forty four SD rats (270-450 g, male) were used in this study. Fourteen animals were employed for the measurement of the middle ear cavity. According to the estimation, the overall volumes in left and right ears showed a similar amount (mean ± standard deviation (STD): 50 µl ± 13.09 and 50.71 ± 9.61, respectively). Therefore, a sham or a UL model was constructed by the injection of approximately 50 µl saline or ferric chloride ($FeCl_3$) solution, respectively. Thirty animals were again divided into three groups: 11 sham, 14 right, and 5 left UL models. The addressed behavioral tests were selectively applied in the UL models, and the number of animals for each symptom was summarized in Table 1, indicating the unilateral vestibular dysfunction. For example, the symptom of spontaneous nystagmus (SN) was observed in 7 right UL and 3 left UL animals, and half of UL models (10/19, 52.63%) showed SN in overall. Another symptom, like tail-hanging, appeared in most UL models (15/19, 78.95%), showing a

relatively high percentage in the population. As expected, the sham group had few symptoms related with the unilateral vestibular dysfunctions in the static and the dynamic tests. Figure 1 illustrated the schematic overview of the experimental procedures. In short, the models were constructed by UL with $FeCl_3$. Once the animals were awakened, some selected behavioral tests were applied to assess the unilateral vestibular dysfunction. Following the tests, the neuronal recording was performed to identify the directional preference.

The relation between the degrees of head deviation (HD) and skewed deviation (SD) was presented depending on the sides of lesion (gray and black for the left and the right UL, respectively) (Figure 2A). Both symptoms were observed in most UL models (14/19, 70.68%, Table 1), and the circles indicated the ocular and the head displacements by UL. In two models, no head tilt was observed after right UL despite the existence of SD, and another two models had no change in SD with the existence of HD. Based on the results, the head rolled to the right by the right UL while it did to the left by the left UL. Total range of HD was between 6.12 and 42.07 deg (mean ± STD: 23.49±10.76 deg), specifically, 14.4-42.07 deg and 6.12-39.43 deg by the left and right UL, respectively. In addition to HD, the neck was often bent laterally after UL. SD was an effective clinical indicator of unilateral vestibular lesion, and this symptom normally appeared in early phase of the behavioral responses. The right UL also induced the ocular displacement, causing the right eye to downward and the left eye to upward direction, and the opposite ocular displacement was produced by the left UL. Due to the displacement, SD resulted in the clockwise and the counter-clockwise rotation by the right and left UL, respectively. Compare with the head tilt, SD was small (mean ± STD: 5.58 ± 2.29 deg), and there was little difference between SD of the right and the left UL (5.76 ± 2.74 deg and 5.27 ± 1.79 deg, respectively). Other static responses were also selectively examined, and the results supported the unilateral vestibular dysfunction. In particular, paw distance (PW) showed the asymmetry limb positions after UL. In the examination using 6 selected UL models, the width between two paws of the front or the hind legs changed, and the alteration in PW was evident at the hind side (Figure 2B). In the front paws, PW rarely changed after UL while that in the hind side increased (53.9%, 7/13), generating a clear separation after UL. The unilateral vestibular dysfunction by UL was further demonstrated by the dynamic behavioral responses. Using the rota-rod test, the walking time on the rolling rod significantly decreased after UL (Figure 2C). The walking time before and after UL ranged from 44 to 335 second (mean ± STD: 208.5 ± 99.56) and 1 to 77 second (13.23 ± 20.42), respectively. The tail-hanging (15/19, 78.95%) and the rotational motion (12/19, 63.16 %) were provoked after UL. The rotational direction in the tail-hanging was headed to the counter-clockwise after the right UL and the clockwise after the left UL. In an open space, the movement of the models showed the animals after UL headed to the side of lesion.

Following the model confirmation by the behavioral tests, the neuronal recording was conducted, and total 77 neuronal responses were recorded, originating from the otolith. Based on the activities in instantaneous firing rates (IFR), all responses were classified as the ipsi- and contra-preferred groups. As shown in two otolith-related examples, the ipsi-preferred neuron increased its IFR as the head linearly translated to the ipsi (right) direction while the contra-preferred neuron increased its IFR by the contra

(left) movement of the head (Figure 3). The head was translated with a speed of ±21.18 cm/s, and the positive and the negative areas represented the ipsi- and the contra-direction, respectively. The positive synchronization between the head velocity and the IFRs identified the ipsi-preferred neuron (Figure 3A), and the negative one implied the contra-preferred neuron (Figure 3B). All neuronal responses were classified by behavioral models as well as the directional preference: 20 (contra-: 13 & ipsi-: 7) from the left UL, 35 (15 & 20) from the sham, and 22 (3 & 19) otolith-related neurons from the right UL (Table 2). As shown in the population, the overall numbers of neuronal responses from the left and the right UL showed no difference ($p=0.561$, Binomial Cumulative Distribution (BCD)). An additional division was conducted for the separation of the pure neurons (responding to linear translation only) and the convergent neurons (responding to horizontal rotation and linear translation). The specific numbers of neurons for each group were summarized in Figure 4 (percentage) and Table 2 (number). In left UL models, the labyrinthectomy generally induced the dominance of the contra-preference by 13 (65%) neurons ($p=0.058$, BCD), and the dominance was significantly led by the convergent neuron (8/9, 89%) ($p=0.002$, BCD). On the other hand, the right UL dominantly generated the ipsi-preference (19/22) in the neuronal responses ($p=6.056\times10^{-5}$, BCD), also leading the ipsi-dominance by the convergent neurons (100%). In sham, there was little difference in the numbers for the ipsi- and the contra-preferred neurons ($p=0.155$, BCD).

Discussion

This study investigated the directional preference in the otolith-related neuronal responses before and after UL as well as a normal condition (sham). Based on the current observations, the biased directional preference was constructed depending on the side of lesion, and the convergent neurons led the dominance in the directional preference. Due to the switched dominance in the directional preference, the unilateral vestibular loss by UL was the key to change the dominance of the directional preference.

Dominant driving force of directional preference

During the head linear translation, the directional preference was primarily driven by the otolith-related neurons, and its balance was disintegrated after UL. Considering the altered dominance in the directional preference after UL, it was also explained that the directional preference was closely related with the incoming neural information from both sides of otolith organs. According to our results, the loss of neural information from one side biased to the same direction. Under normal conditions (sham model), the distribution of the ipsi- and the contra-preferred neurons was even, and the pure neurons were the major group ($p<<0.001$, BCD). Under the same condition, there was no significant dominance in the directional preference. After UL, however, the directional preference became biased, and the result was emphasized in the convergent neurons (Figure 4 & Table 2). After the left UL, the contra-preferred was dominant, and the ipsi-preferred was main direction after the right UL ($p<0.004$, BCD). Even though the neuronal type in sham group indicated the opposite distribution compared with that after UL, the convergent neurons mainly governed the directional preference regardless of the side of lesion. The same consequence was

driven by all convergent neurons in the sham and UL models, and, thus, the main diving force for the directional preference was induced by the information of the convergent neurons.

Unlike our current data in sham, the neuroanatomical basis suggested that the otolith neurons dominantly had contra-preferred direction. However, few direct examinations on the dominant directional preference had been performed. From the aspect of the neural excitation, the right UL model lost the concurrent neural information from the right labyrinth, and it received the incoming stimulation only through the left side of the CP [11,18,22,23]. During the ipsilateral translation after right UL, the hair cells initiated the excitation of the vestibular afferent neurons by the pars medialis in the left side, projecting on the right side of VN through CP [14,15]. Therefore, the neural recording on the right side of VN showed the increased neuronal activity as the head moved toward right direction while the induced neural activity was dominant to the left VN. The serial activities of the utricular afferents were mainly governed by the hair cells in the pars medialis, which located at the opposite side of labyrinthectomy. Also, it was highly expected that the neural information from the pars lateralis was suppressed because of the superiority of the pars medialis in the population, and that was why there were only several contra-preferred neurons.

Model confirmation based on behavioral responses

Chemical labyrinthectomy eliminated the hair cells, and it caused the asymmetric neural activity in VN [24-26]. Furthermore, the chemical labyrinthectomy has been known an easier and more efficient approach than the surgical method [27-30]. Due to the abnormal behavioral responses following the unbalanced neural information, various behavioral tests were adopted with no animal sacrifice for the model evaluation [31]. A previous study reported that a toxic (ex. sodium arsanilate) injection caused SN and HD [32], and the injection of streptomycin also induced SN and HD within 12 hours [33,34]. Some experimental results demonstrated that an abnormal ocular symptom, called ocular tilt reaction, was caused by the damages on the utricle [14,35-37]. These accumulative results suggested that the head and the ocular responses were the critical indicators for the unilateral vestibular dysfunction, and the examination on the responses was a reasonable method for the model evaluation [28,37,38]. In addition, the limb asymmetry after UL was also previously investigated during the functional recovery and neurogenesis [28]. In this study, the neural recording was followed by the model confirmation, and the behavioral tests were relevant with no animal sacrifice. Previously approved tests were included for the evaluation, and the analysis for the PW was newly developed to identify the continuously changing symmetry in the limb. The obtained results in static and dynamic tests indicated that the models constructed the unilateral vestibular dysfunction by UL, and the assessments were shown in the analyzed consequences. Nevertheless, there was a limit to show how much damage was caused by $FeCl_3$ injection. According to a previous histological study, neither chemical nor the surgical labyrinthectomy conducted a complete removal of the vestibular hair cells [31]. However, the purpose for the evaluation was to investigate the unbalanced vestibular function after UL and the alteration in the directional preference in the neuronal activity. Thus, the behavioral tests were suitable for the evaluation for this study.

Conclusion

The directional preference of the otolith-related neurons in VN was investigated using the chemical UL models as well as the normal condition. Our current study demonstrated that UL caused to block the delivery of neural information originated in otolith to the central area (VN), and the consequences of UL were estimated by the skewed distribution of directional preference as well as the abnormal behaviors. As indicated in previous neuroanatomical studies, the neural link of two separated labyrinths maintained the balanced directional preference, but its interruption by UL biased the directional preference. Agreeing with the previous evidence, the directional preference of the otolith-related neurons in VN was biased to the ipsi- or the contra-direction depending on the side of lesion. Especially, the bias in the directional preference was clearly observed in the convergent neurons which received the neural information by the head rotation and the linear translation. In conclusion, the directional preference of the otolith-related neurons in VN was evenly distributed under a normal condition, and the effect by UL was relatively significant on convergent neurons.

Methods

All experimental procedures and the laboratory animal care in this study were verified and approved by Inha University Animal Ethics Committee. All animals (SD rats, male) were provided by an animal provision company (Oriental Bio corp., Korea).

Animal preparation

Unilateral labyrinthectomy (UL) was performed by intratympanic injection of ferric chloride ($FeCl_3$) using rodents (SD rats, male). For the injection, a syringe (0.5 mm-diameter needle) was inserted through the tympanic membrane until its tip encountered the middle-ear ossicles. Once positioned, the needle was slightly pulled back, and the injection was conducted. To estimate a proper amount of the $FeCl_3$ solution (mixture of 0.97 g $FeCl_3$ and 1.4 ml saline), we initially used saline to assess the volume of the middle ear cavity. An animal was anesthetized by the intramuscular injection of a mixed solution (1.3 ml/kg) of Ketamine (1 μl/g) and Xylazine (0.33 μl/g). Following the anesthesia, saline was injected until it was emerged back through the tympanic membrane. Once the backward flow of saline was observed, the injection was ceased, and the injected volume was measured. Determining the averaged amount based on multiple measurements, the same volume of $FeCl_3$ solution was applied to an animal for a UL model. After constructing the UL model, the animal was in a resting stage until it was recovered from the anesthesia.

Behavioral test

Both tests for static and dynamic symptoms were conducted immediately after the animals were fully awaken, which was approximately 0.5-1 hour later from the moment of $FeCl_3$ injection. Also, the behavioral tests generally lasted for an hour to complete both types of tests. Thus, all behavioral tests were finalized within 2 hours after $FeCl_3$ injection.

Static symptoms

The static symptoms were observed in the absence of the head movements. Spontaneous nystagmus (SN), skewed deviation (SD), head deviation (HD), and paw distance (PW) were used as the critical indicators for the unilateral vestibular dysfunction. SN was the rhythmical ocular movement with a rapid phase toward the opposite side of the lesion. SD was the horizontal misalignment by the ocular displacements, defined as the tilted degree between a horizontal line and the imaginary line by both eyes. HD was the vertical misalignment of the head, defined as the tilted degree between a vertical line and the imaginary line by the head. PW was estimated by the distance between two front or hind paws. For the PW measurement, the animal was placed in a transparent box right after its awakening, and the paw positions were identified for at least 30 sec. Using the recorded positions, PW was calculated before and after UL.

Dynamic symptoms

The dynamic symptoms were examined in the animals' free head movements. Three different behavioral responses, such as rota-rod test, tail-hanging, and rotational direction, were used for identifying the unilateral vestibular dysfunctions. The rota-rod test has been commonly used to estimate the animal's motor function by measuring the time that the animal was maintaining on the rolling rod (5.9 cm/sec). Using the tail-hanging test, it was examined if the body was spun, which rarely happen before UL. In an open space, the animal's directional movement was also examined to identify the rotational direction, depending on the side of the vestibular lesion. All behavioral tests were conducted to identify the unilateral vestibular dysfunction after UL.

Extracellular neural recording

Following the behavioral tests, the animal was re-anesthetized by the same method (see **Animal preparation**). Once the animal was fully anesthetized, it was placed on the motorized stereotaxic apparatus (NEUROSTAR, Germany) to fix its head. The overall neural recording process followed our previous methodological approach [19-21] for approximately 3 hours. In short, surgically removed its scalp, the superior surface of the skull was exposed. On the surface, the lambda was designated as a center, and the hole (2.0 mm diameter) for a recording electrode (5 M**Ω**, A-M system, US) was opened (generally, 3.0 mm posterior and 2.0 mm lateral away from the center). Due to the recording position, the right side of the animal was defined as the ipsilateral direction. The neuronal activities were explored by advancing the recording electrode, and they were tested by the kinetic stimuli, such as a horizontal rotation and the linear translation following the x- axis (ipsi- & contra-lateral). Based on the responses to the kinetic stimulation, the neurons were classified as a pure otolith or a convergent (otolith+canal-related) neuron. The pure otolith neuron showed a neuronal response only to the linear translation while the convergent neuron responded to both kinetic stimuli. The neuronal responses to the stimulation were recorded with the sampling rate of 40 kHz in OmniPlex D system (Plexon, TX) after amplified and filtered (bandpass 0.5-3 kHz). All the recordings were performed under the anesthetized condition.

Data analysis

Behavioral tests were composed of four types of static symptom and three types of dynamic symptom tests. For PW, the measured distances were executed off-line using a user code written in MATLAB (MathWorks, USA). The distances were presented in a bar chart to identify a possible width by two feet, and the normal width was assessed by measuring the largest and the smallest values (1-15cm for front & 1-10cm for hind). The final value was presented by a range, instead of averaged values. As briefly explained in Behavioral test, SD and HD were examined by the misalignments compared with the horizontal and vertical lines, and they were assessed by the altered lines in the ocular and the head displacements, respectively. The tail-hanging, the rotational motion, and SN were confirmed based on the observation, and the rota-rod test was analyzed using the measured times (mean ± standard deviation).

The directional preference was determined by the neuronal response to the kinetic stimulation following the x-axis (passive inter-aural translation), which was originated from the utricle. During the repeated right- or leftward linear translation, IFR of the neuron was evaluated; if IFR increased as the head was linearly translated to the right direction, the neuron was identified as ipsi-preferred unit. The contra-preferred neuron increased its IFR as the head was linearly translated to the left direction. In addition, the neuronal information responding to the horizontal rotation was examined to demonstrate if the recording response was originated from a pure or a convergent neuron.

To assess a statistical significance, Binomial Cumulative Distribution (BCD) function was applied. As all compared groups were one or the other, BCD tested if the different numbers in two groups were statistically similar. Based on this test, the bias was determined between the groups with different directional preference; the ipsi- and the contra-preferred neurons.

Abbreviations

BCD: Binomial Cumulative Distribution

CP: Commissural Pathway

$FeCl_3$: Ferric Chloride

HD: Head Deviation

IFR: Instantaneous Firing Rate

PW: Paw Distance

VN: Vestibular Nucleus

SD: Skewed Deviation

SN: Spontaneous Nystagmus

STD: Standard Deviation

UL: Unilateral Labyrinthectomy

Declarations

Ethics approval and consent to participate

All procedures and experiments as well as principles of laboratory animal care were inspected and approved by the Animal Ethics Committee at Inha University.

Consent for publication

No individual person’s data were included in this study.

Availability of data and materials

The data in the current study are not publicly available, but they may be available on reasonable request.

Competing interests

No potential competing interest relevant to this article was reported.

Funding

This research was supported by Basic Science Research Program through the National Research Foundation of Korea (NRF) funded partially by the Ministry of Education (2018R1A6A1A03025523 & 2019R1I1A1A01041450).

Authors' contributions

Nguyen Nguyen (NN) and Gyutae Kim (GK) designed the study and conducted experiments. NN and GK drafted the manuscript, and GK finalized editing the ma. NN and GK worked on the figure generation, together. Kyu-Sung Kim (KSK) and GK provided the funding resources to support this study. KSK also helped to develop its quality by suggesting some medical advices. All authors read and approved the final manuscript.

Acknowledgements

Not applicable

References

1. Angelaki DE, Cullen KE. Vestibular System: The Many Facets of a Multimodal Sense. Ann. Rev. Neurosci. 2008;31(1):125-150.

2. Borel L, Lopez C, Péruch P, Lacour M. Vestibular syndrome: A change in internal spatial representation. Neurophysiol. Clin./Clin. Neurophysiol. 2008;38(6): 375-389.
3. Lacour M, Dutheil S, Tighilet B, Lopez C, Borel L. Tell Me Your Vestibular Deficit, and I'll Tell You How You'll Compensate. Ann. NY Acad. Sci. 2009;1164(1):268-278.
4. Péricat D, Farina A, Agavnian-Couquiaud E, Chabbert C, Tighilet B. Complete and irreversible unilateral vestibular loss: A novel rat model of vestibular pathology. J. Neurosci. Meth. 2017;283:83-91.
5. Mitchell DE, Della Santina CC, Cullen KE. Plasticity within excitatory and inhibitory pathways of the vestibulo-spinal circuitry guides changes in motor performance. Sci. Rep. 2017;7(1):853. doi: 10.1038/s41598-017-00956-5.
6. Yoder RM, Taube JS. Head direction cell activity in mice: Robust directional signal depends on intact otolith organs. J. Neurosci. 2009;29(4):1061-1076.
7. Kasri M, Picquet F, Falempin M. Effects of unilateral and bilateral labyrinthectomy on rat postural muscle properties: the soleus. Exp. Neurol. 2004;185(1):143-153.
8. Dakin CJ, Héroux ME, Luu BL, Inglis JT, Blouin JS. Vestibular contribution to balance control in the medial gastrocnemius and soleus. J. Neurophysiol. 2004;115(3):1289-1297.
9. Chan YS, Cheung YM. Response of otolith-related neurons in bilateral vestibular nucleus of acute hemilabyrinthectomized cats to off-vertical axis rotationsa. Ann. NY Acad. Sci. 1992;656(1):755-765.
10. Hitier M, Besnard S, Smith PF. Vestibular pathways involved in cognition. Front. Integ. Neurosci. 2014;8:59.doi: 10.3389/fnint.2014.00059.
11. Newlands SD, Abbatematteo B, Wei M, Carney LH, Luan H. Convergence of linear acceleration and yaw rotation signals on non-eye movement neurons in the vestibular nucleus of macaques. J. Neurophysiol. 2018;119(1):73-83.
12. Lowenstein O, Sand A. The individual and integrated activity of the semicircular canals of the elasmobranch labyrinth. J. Physiol. 1940;99(1):89-101.
13. Lindeman HH. Studies on the morphology of the sensory regions of the vestibular apparatus. Ergeb. Anatom. Entwick. 1969;42:1-113.
14. Carey JP, Della Santina CC. Principles of Applied Vestibular Physiology. In: Flint PW, et al., Editors, Cummings otolaryngology-Head and neck surgery, St. Louis: Elsevier; 2014. p. 2494-2524.
15. Fitzpatrick RC, Day BL. Probing the human vestibular system with galvanic stimulation. J. App. Physiol. 2004;96(6):2301-2316.
16. Fernandez C, Goldberg JM. Physiology of peripheral neurons innervating otolith organs of the squirrel monkey. I. Response to static tilts and to long-duration centrifugal force. J. Neurophysiol. 1976;39(5): 970-984.
17. Loe PR, Tomko DL, Werner G. The neural signal of angular head position in primary afferent vestibular nerve axons. J. Physiol. 1973;230(1):29-50.

18. Newlands SD, Lin N, Wei M. Responses of non-eye movement central vestibular neurons to sinusoidal horizontal translation in compensated macaques after unilateral labyrinthectomy. J. Neurophysiol. 2014;112(1):9-21.
19. Kim G, Kim KS, Lee S. The integration of neural information by a passive kinetic stimulus and galvanic vestibular stimulation in the lateral vestibular nucleus. Med. Biol. Eng. Comput. 2017;55(9):1621-1633.
20. Kim G, Kim KS, Lee S. Non-associative learning processes in vestibular nucleus. Med. Biol. Eng. Comput. 2018;56(10):1841-1851.
21. Kim G, Lee S, Kim KS. Dominant parameter of galvanic vestibular stimulation for the non-associative learning processes. Med. Biol. Eng. Comput. 2020; doi: 10.1007/s11517-019-02117-4. [Epub ahead of print].
22. Lannou J, Cazin L, Hamann KF. Response of central vestibular neurons to horizontal linear acceleration in the rat. Pflüg. Arch. 1980;385(2):123-129.
23. Xerri C, Gianni S, Manzoni D, Pompeiano O. Central compensation of vestibular deficits. I. Response characteristics of lateral vestibular neurons to roll tilt after ipsilateral labyrinth deafferentation. J. Neurophysiol. 1983;50(2):428-448.
24. Curthoys IS. Vestibular compensation and substitution. Curr. Opin. Neurol. 2000;13(1):27-30.
25. Darlington CL, Lawlor P, Smith PF, Dragunow M. Temporal relationship between the expression of Fos, Jun and Krox-24 in the guinea pig vestibular nuclei during the development of vestibular compensation for unilateral vestibular deafferentation. Brain Res. 1996;735(1):173-176.
26. Lacour M, Helmchen C, Vidal PP. Vestibular compensation: the neuro-otologist's best friend. J. Neurol. 2016;263(Suppl 1):54-64.
27. Bostanci MÖ, Bagirici F. Blocking of L-type calcium channels protects hippocampal and nigral neurons against iron neurotoxicity the role of L-type calcium channels in iron-induced neurotoxicity. Intern. J. Neurosci. 2013;123(12):876-882.
28. Shaabani M, Lotfi Y, Karimian SM, Rahgozar M, Hooshmandi M. Short-term galvanic vestibular stimulation promotes functional recovery and neurogenesis in unilaterally labyrinthectomized rats. Brain Res. 2016;1648(Pt A):152-162.
29. Vignaux G, Chabbert C, Gaboyard-Niay S, Travo C, Machado ML, Denise P, Comoz F, Hitier M, Landemore G, Philoxène B, Besnard S. Evaluation of the chemical model of vestibular lesions induced by arsanilate in rats. Toxicol. App. Pharmacol. 2012;258(1):61-71.
30. Willmore LJ, Hiramatsu M, Kochi H, Mori A. Formation of superoxide radicals after FeCl3 injection into rat isocortex. Brain Res. 1983;277(2):393-396.
31. Lee J, Kim M, Park B. Vestibular end organ injury induced by middle ear treatment with ferric chloride in rats. Hum. Exper. Toxicol. 2017;36(2):146-159.
32. Kim MS, Kim JH, Jin YZ, Kry D, Park BR. Temporal changes of cFos-like protein expression in medial vestibular nuclei following arsanilate-induced unilateral labyrinthectomy in rats. Neurosci. Lett. 2002;319(1):9-12.

33. Horiike O, Shimogori H, Yamashita H. Effect of edaravone on streptomycin-induced vestibulotoxicity in the guinea pig. Laryngoscope. 2004;114(9):1630-1632.
34. Shimogori H, Yamashita H. Peripheral vestibular disorder induced by (±)-α-amino-3-hydroxy-5-methyl-isoxazole-4-propionic acid (AMPA). Neurosci. Lett. 2004;371(1):69-72.
35. Brodsky MC, Donahue SP, Vaphiades M, Brandt T. Skew deviation revisited. Surv. Ophthalmol. 2006;51(2):105-128.
36. Hitier M, Besnard S, Vignaux G, Denise P, Moreau S. The ventrolateral surgical approach to labyrinthectomy in rats: anatomical description and clinical consequences. Surg. Radiol. Anat. 2010;32(9):835-842.
37. Smith PF, Curthoys IS. Mechanisms of recovery following unilateral labyrinthectomy: a review. Brain Res. Rev. 1989;14(2):155-180.
38. Sirkin DW, Precht W, Courjon JH. Initial, rapid phase of recovery from unilateral vestibular lesion in rat not dependent on survival of central portion of vestibular nerve. Brain Res. 1984;302(2):245-256.

Tables

Table 1. The number of animals for each symptom at right or left UL model

Symptom	Right UL model	Left UL model	Total
SN	7	3	10
SD	9	5	14
HD	9	5	14
PD	8	5	13
rota-rod	7	4	11
rotational motion	8	4	12
tail hanging	13	2	15

Abbreviation: **UL**: unilateral labyrinthectomy, **SN**: spontaneous nystagmus,

SD: skew deviation, **HD**: head deviation, **PD**: paw distance

Table 2. The number of contra- and ipsi-preferred neuron in each group

	Left UL		Sham		Right UL	
preferred direction	contra-	ipsi-	contra-	ipsi-	contra-	ipsi-
pure otolith	5	6	11	15	3	11
canal + otolith	8	1	4	5	0	8
total	13	7	15	20	3	19

Abbreviation: **UL**: unilateral labyrinthectomy,

contra-: contra-preferred direction, **ipsi-**: ipsi-preferred direction,

Pure otolith: responding to passive inter-aural translation only,

Canal+otolith: responding to horizontal rotation and passive inter-aural translation

Figures

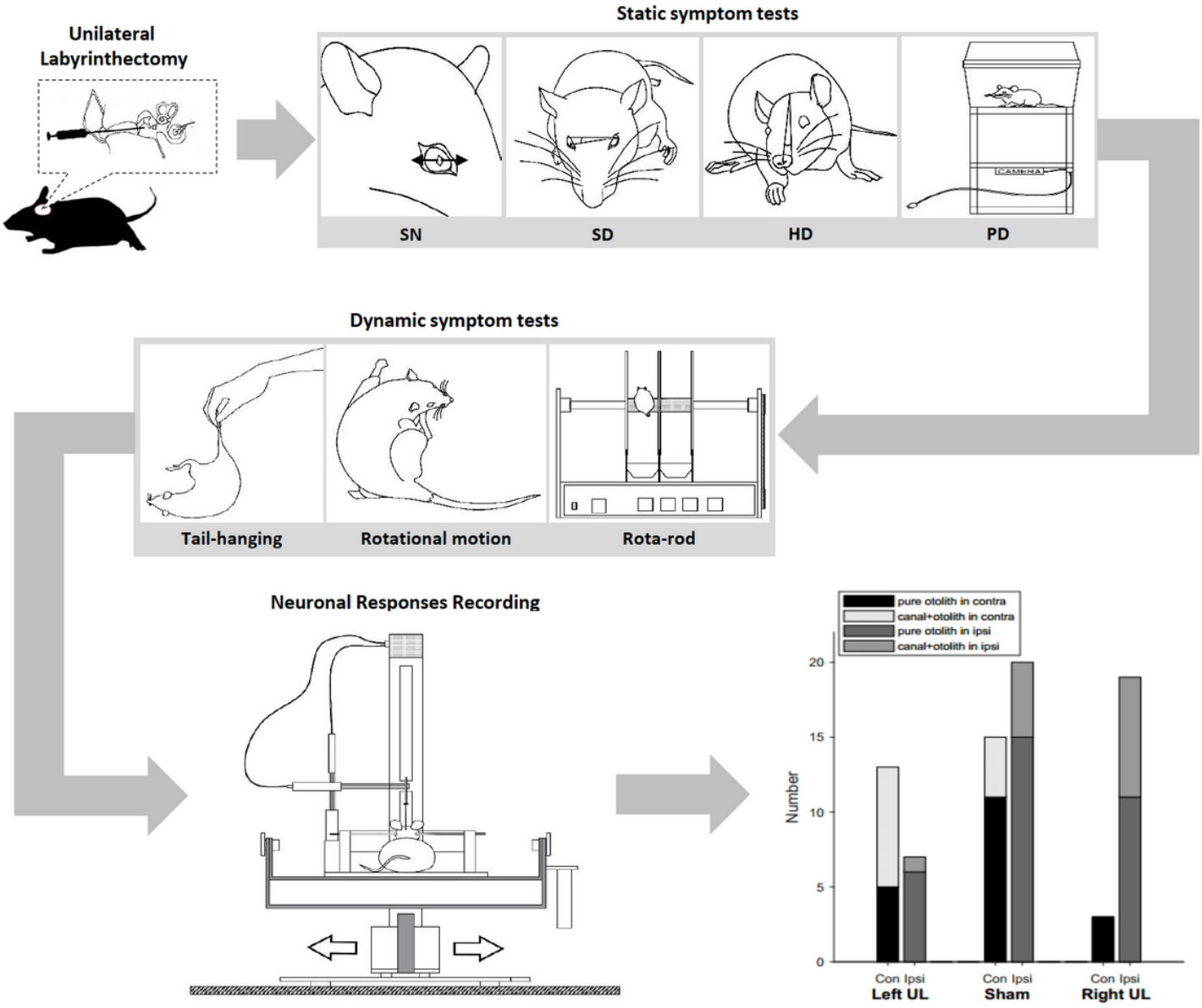

Figure 1

Schematic overview of experimental procedure. Unilateral labyrinthectomy (UL) model was induced by an intratympanic FeCl3 injection, and the animal underwent two types of behavioral tests, static and dynamic symptom tests. Once the model was confirmed, extracellular neural recording was conducted. During the online neural recording, the otolith-related neurons were identified, and their directional preference was determined. The directional preference was examined if there was any relation to the effect by UL and its lesion location.

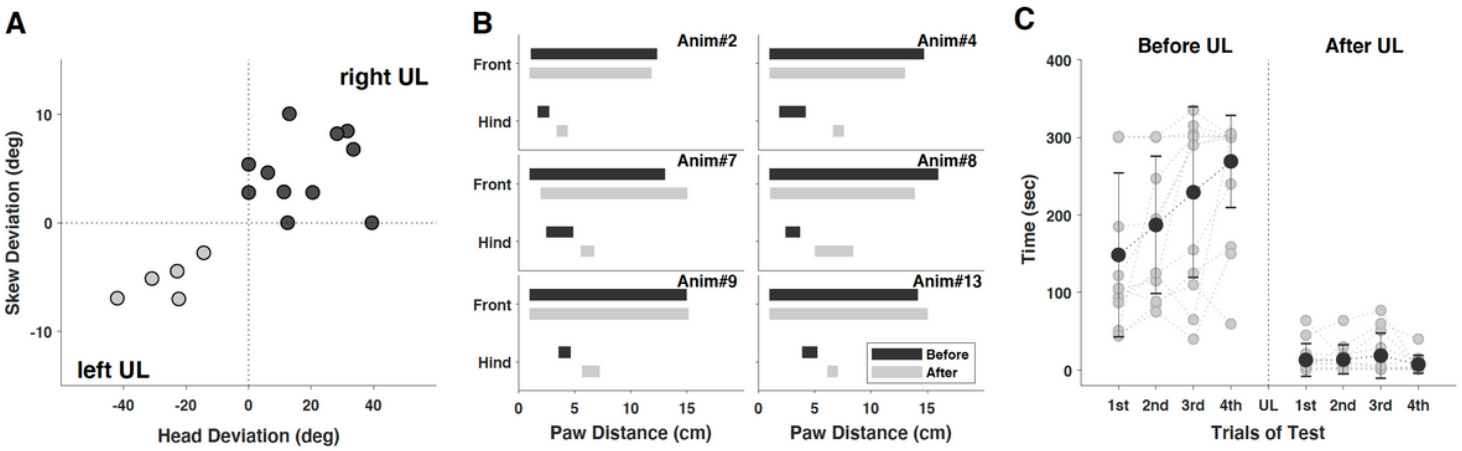

Figure 2

Behavioral Responses. A, Relation between the degrees of the head (HD) and the ocular skew deviation (SD). The black and the gray circles indicated by HD and SD after right and left UL, respectively. Some animals showed no HD (2) or SD (2), locating at the dotted line. B, Front and hind paw distances from 6 selected animals before and after UL. Each bar represented the range of paw distance. C, Rota-rod tests before and after UL. For each condition, animals were tested in 4 trials, and the performing time on the rolling rod decreased after UL.

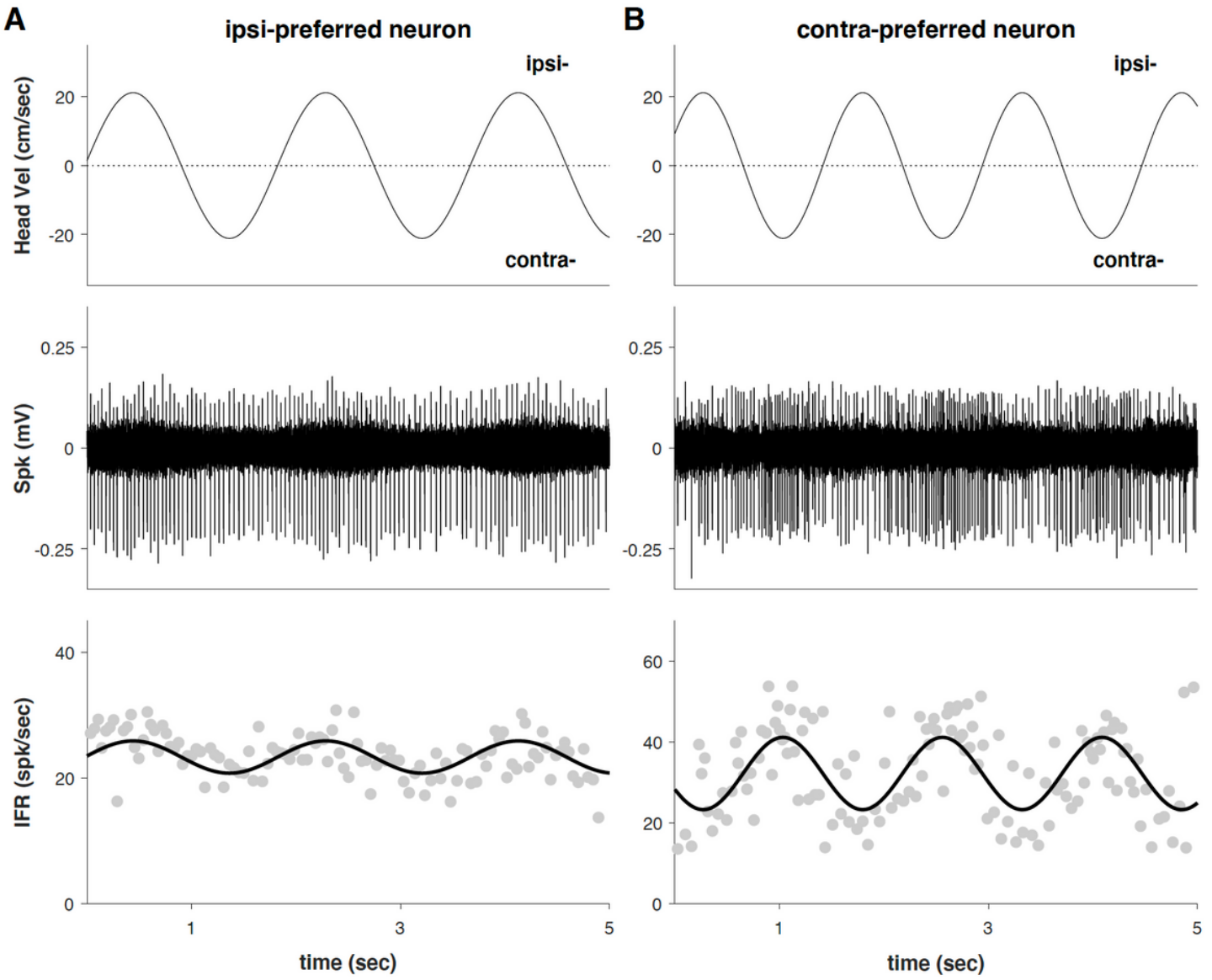

Figure 3

Neuronal examples responding to head velocity. Two neurons were selected to show their responses to the given kinetic stimulation. A, Example of ipsi-preferred neuron. The sinusoidal wave represented the head velocity (amplitude: ±21.18 cm/s). As labeled, the upper in the subplot indicated the ipsi-, and the lower space did the contra-direction (A, top). Depending on the supplied kinetic stimulation, the concurrent neuronal spikes were recorded (A, middle). Their corresponding instantaneous firing rates (IFR, gray dot) were computed and presented to show their relation with the given stimulation (A, bottom). To emphasize the changes of IFR, a curve fitting was used to find a wave for the distribution of IFR, and a curved line in black was applied. B, Example of contra-preferred neuron. The basic format of subplots was exactly same as that in A. The difference was the neuronal response to the head velocity. Unlike the case in the ipsi-preferred neuron, this neuronal IFR increased as the motional direction shifted to the contra-direction.

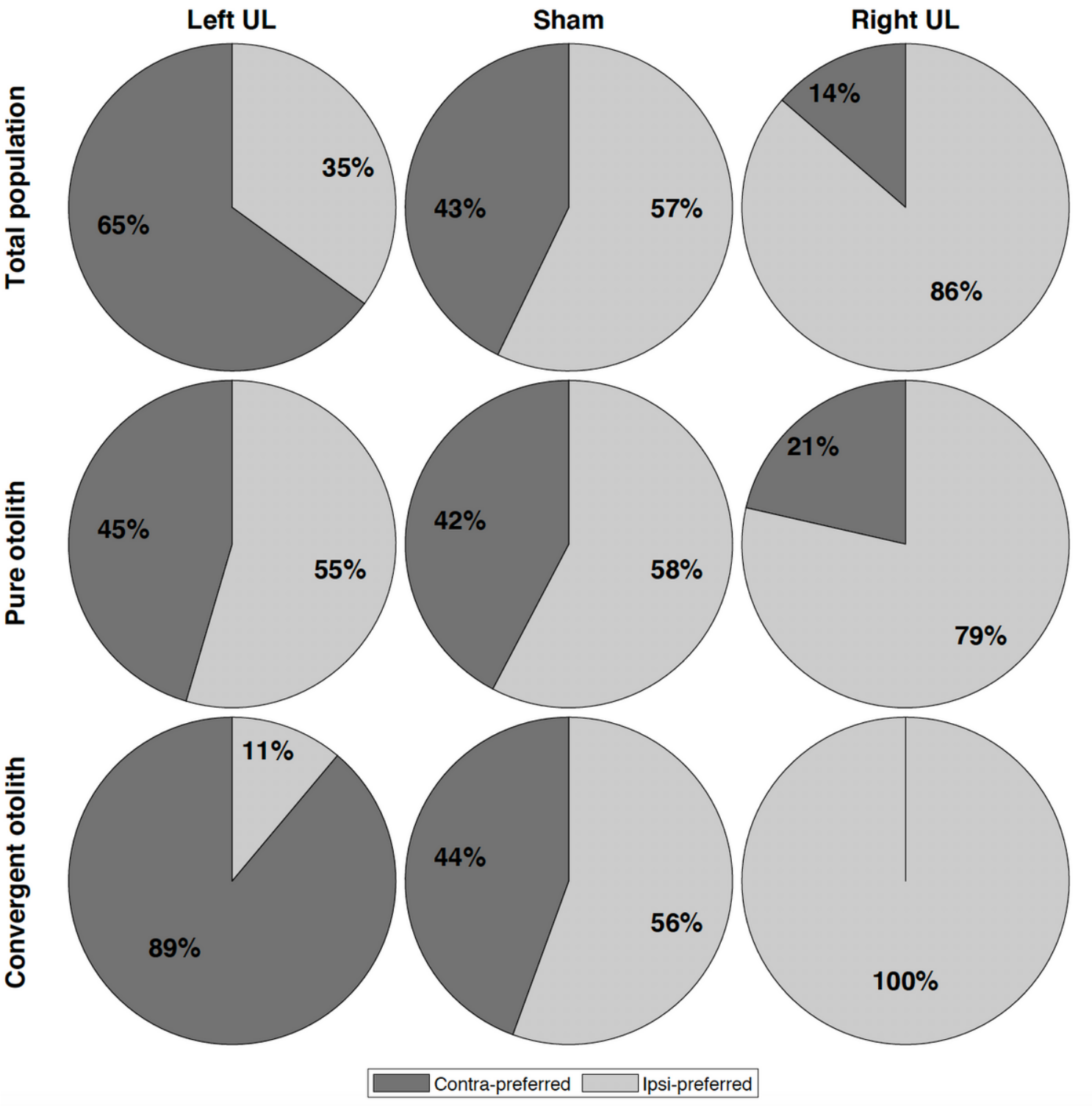

Figure 4

Population by lesion location. Specified populations were presented in pie charts. Total population was divided into three sub-groups; left unilateral labyrinthectomy (UL), sham, and right UL (1st row). In each group, the neurons were again classified as the pure otolith-related (OR, receiving otolith input only) (2nd row) and the otolith+canal-related (OCR, receiving both canal and otolith input) units (3rd row), using the responses to the passive inter-aural translation. In the sham, the population in both OR and OCR showed a similar distribution for the ipsi- and the contra-preferred neurons. On the other hand, the population after

UL biased to the contra-preferred under the left UL and the ipsi-preferred after right UL. Both biased tendencies were led by the changed population in the OCR.

Supplementary Files

This is a list of supplementary files associated with this preprint. Click to download.

- SubmissionNC3RsARRIVEGuidelinesChecklist.docx